Quantitative Analysis of Artifacts in Volumetric DSA: the Relative Contributions of Beam Hardening and Scatter to Vessel Dropout Behind Highly Attenuating Structures

James R. Hermus[a,b], Timothy P. Szczykutowicz[a,c], Charles M. Strother[c], Charles Mistretta[a,b,c]
[a]Department of Medical Physics, University of Wisconsin-Madison, WI 53705
[b]Department of Biomedical Engineering, University of Wisconsin-Madison, WI 53706
[c]Department of Radiology, University of Wisconsin-Madison, WI 53792

Motivation

In 4D-DSA image reconstruction [1, 2] vessel dropout was observed due to highly attenuating anatomy, such as large aneurysms and dental implants. In this work, we have developed a method for acquiring DSA projections that models both the polychromatic nature of the x-ray spectrum and the x-ray scattering interactions to investigate this problem. Maximum intensity projection (MIP) images of 4D-DSA reconstructions display two vessel dropout cases, as shown in Figures 1.

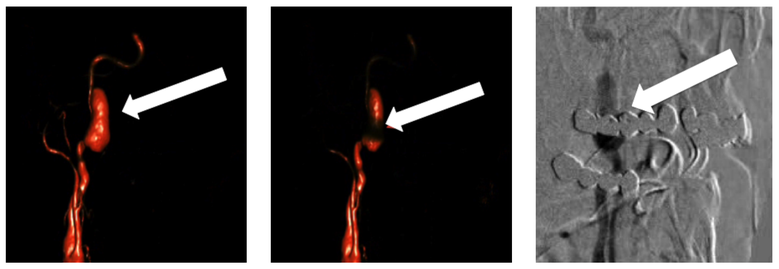

(a) (b) (c)

Figure 1: (a) Arrows indicate the portion of the vessel that experiences contrast degradation. (a) 4D-DSA reconstruction of an aneurysm in the carotid artery with no signal loss. (b) 4D-DSA volume reconstructed using a projection in which dental implants are interfering with the signal from the aneurysm. (c) A projection image after digital subtraction at the same view angle as image (b). Some of the anatomy is visible due to a slight misregistration and one can clearly observe that the dental implants are causing the loss of vessel contrast.

Why Create Digital Phantoms?

When analyzing clinical data and humanoid phantoms the variation in tissue and vessel thickness made the acquisition of large clearly defined ROIs with uniform thickness impossible. We constructed digital phantoms with large clearly defined regions containing iodine contrast, bone, soft issue, titanium (dental implants) or combinations of these materials. As the regions containing the materials were large and rectangular, when the phantoms were forward projected, the projections contained uniform regions of interest (ROI) and enabled accurate vessel dropout analysis.

Using a Monte Carlo simulation and a forward projector we were able to produce projections with and without scatter. Using a monochromatic beam vs. a polychromatic beam we could turn on and off beam hardening. These acquisition methods allowed us to create five DSA images as seen in Table 1.

Image	spectrum type	primary signal	scatter singal
Ideal	monochromatic	X	
Beam Hardening	polychromatic	X	
Monoscatter	monochromatic		X
Polyscatter	polychromatic		X
BH and Scatter	polychromatic	X	X

Table 1: This table outlines how each different DSA projection was constructed. As we have the ability to turn both beam hardening and scatter on and off, we can quantify the effect of these phenomena on vessel dropout separately.

Methods

Digital phantoms were constructed containing regions representing bone, soft tissue, contrast, and titanium, which presented large clearly defined ROIs. All linear attenuation coefficient data and x-ray spectra were generated using the spektr [3] software tool kit. This tool kit is based on the TASMIP [4] algorithm developed by Boone and Seibert.

The 3D volumes were used in a MC simulation to generate the scatter signal for the image. A MC simulation of x-ray transport in a graphic processor unit (GPU) with Compute Unified Device Architecture (CUDA) was used [5]. This accelerated Monte Carlo simulation was developed by Badal and Badano, it is known as MC-GPU. Each simulation was run for approximately one hour, simulating 60.1x107 x-rays. The speed was 172269.24 x-rays per second. The MC-GPU simulates Rayleigh scattering, Compton scattering and photoelectric effect photon interactions. The MC simulation generated two images, a primary and a scatter image.

To generate a DSA forward projection, a forward projection of a mask and fill volume are needed. The mask phantom contains all materials except iodine, as in an actual mask projection there would be no iodine contrast in the vessels. The fill volume will have all materials (including iodine contrast) in the projection. After the forward projections are created, the fill projection can be log subtracted from the mask projections to create a DSA forward projection of the vessels.

Methods Continued

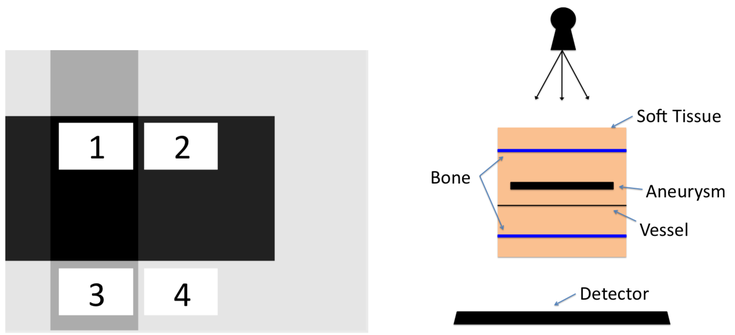

(a) (b)

Figure 2: (a)This is a DSA projection of the phantom designed to simulate the case of a large aneurysm causing vessel drop out. The ROIs used to calculate the contrast are numbered. (b) This is a diagram (not to scale) displaying the way in which the volume was positioned. Each bone region is 4 mm thick, to simulate the thickness of a temporal bone. The large slab of iodine simulates the 11 mm aneurysm in the internal carotid artery and the last block is meant to simulate the vessel with a thickness of 1 mm.

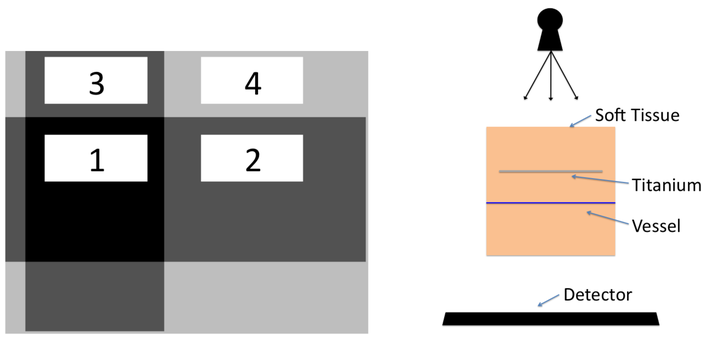

(a) (b)

Figure 3: This is a DSA projection of the phantom designed to simulate Figure 1, the teeth case. (b) This is a diagram (not to scale) displaying the way in which the volume was positioned. The iodine slab with a thickness of 1 mm represents the vessel and the titanium is 2 mm to simulate a dental implant.

Results and Discussion

The vessel contrast was plotted to compare the regions with and without the highly attenuating material. As expected in the ideal projection, without beam hardening and scatter, the contrast from the vessel behind the highly attenuating material was equal to the contrast without the material. It was observed that the monochromatic and polychromatic scatter cases did not produce a substantial difference in contrast. Figure 4 and 5 display the effect the aneurysm and the dental implants have on the contrast produced from the vessel and the images from which the ROIs were averaged.

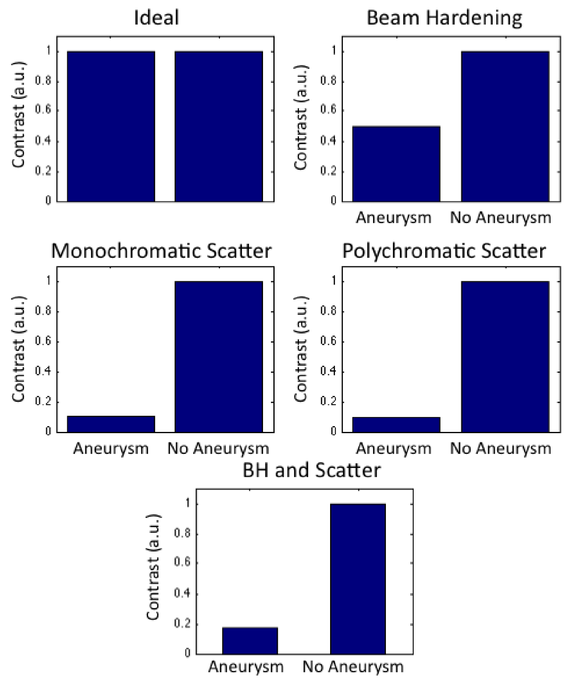

Figure 4: Results created by projecting the volume simulating the Aneurysm case.

Results and Discussion Continued

In the aneurysm case both iodine contrast and a thick temporal bone were present, and in the teeth case there was 2 mm of titanium to simulate a dental implant. The difference in the attenuation of the bone and iodine (see Table 2) versus just the titanium is believed to be the cause of higher vessel contrast degradation in the aneurysm case. The 4 mm temporal bone and the 11 mm of iodine contrast attenuated more x-rays than the 2 mm of titanium. The linear attenuation coefficient of bone, iodine contrast agent and titanium at 62 KeV is 0.5793 mm-1, 9.4468 mm-1 and 3.24 mm-1 respectively. When multiplied by the thickness of each material, 8mm for bone, 11 mm for contrast and 2 mm for titanium, the attenuation in the aneurysm case is 108.55 and the attenuation in the teeth case is 6.48. This demonstrates the substantial difference in attenuation between the aneurysm case and the teeth case.

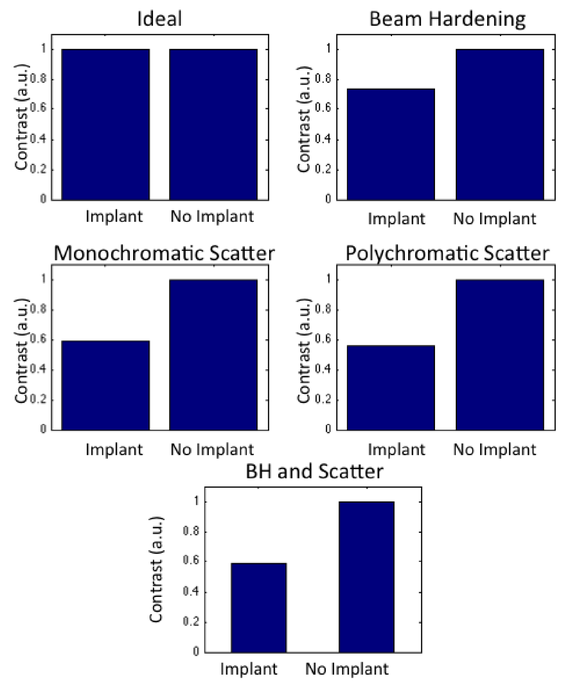

Figure 5: Displays the results from the projection of the volume simulating the Teeth case in Figure 1.

Image Type	Ideal	BH	Monochromatic Scatter	Polychromatic Scatter	BH + Scatter
Aneurysm case	0%	50.5%	89.8%	90.25%	82.9%
Teeth case	0%	26.2%	41.11%	44.2%	41.4%

Table 2: : Displays a table with the percentage of contrast that was lost in each of the four types of projections for the teeth case and the aneurysm case.

New Work

Ultimately a more robust scatter correction/BH needs to be developed. We are working on developing methods aimed at correcting the signals specifically behind highly attenuating structures, areas where current scatter correction methods fail.

Conclusions

This quantitative analysis of the vessel degradation in cases of highly attenuating anatomy suggests that the contrast degradation is primarily due to scatter artifacts, not beam hardening. These results are clear after investigating the combination of a forward projection and Monte Carlo simulations to produce five images: ideal, beam hardening, monochromatic scatter, polychromatic scatter, and beam hardening and scatter.

References

[1] B. Davis, K. Royalty, M. Kowarschik, C. Rohkohl, E. Oberstar, B. Aagaard-Kienitz, D. Niemann, O. Ozkan, C. Strother, and C. Mistretta, "4d digital subtraction angiography: Implementation and demonstration of feasibility," *American Journal of Neuroradiology* , April 2013.

[2] C. A. Mistretta, "Sub-nyquist acquisition and constrained reconstruction in time resolved angiography," *Med. Phys.* **38**, pp. 2975–2984, June 2011.

[3] J. H. Siewerdsen, A. M. Waese, D. J. Moseley, S. Richard, and D. A. Jaffray, "Spektr: A computational tool for x-ray spectral analysis and imaging system optimization," *Med. Phys.* **31**, pp. 3057–3067, Nov. 2004.

[4] J. M. Boonea and J. A. Seibert, "An accurate method for computer-generating tungsten anode x-ray spectra from 30 to 140 kv," *Med. Phys.* **24**, pp. 1661–1670, Nov. 1997.

[5] W. mei Hwu, ed., *GPU Computing Gems Emerald Edition*, no. 978-0-12-384988-5, Elsevier Inc., emerald edition ed., 2011.